



Responsive laminarin-boronic acid self-healing hydrogels for biomedical applications

Adérito J. R. Amaral¹ · Vítor M. Gaspar¹ · João F. Mano¹

Received: 1 February 2020 / Revised: 22 March 2020 / Accepted: 31 March 2020
© The Society of Polymer Science, Japan 2020

Abstract

The precise chemical modification of marine-derived biopolymers provides a unique opportunity for fabricating a toolbox of bioactive (bio)materials with modulated physicochemical and biological properties. Herein, the β -glucan laminarin was functionalized with phenylboronic acid (PBA) moieties that impart chemical reactivity toward diol-containing polymers via boronate esterification. The modification, which involved a two-pot reaction, was successfully confirmed by nuclear magnetic resonance spectroscopy. The resultant biopolymer readily established boronate ester-crosslinked hydrogels with poly(vinyl alcohol) (PVA) within seconds under physiological conditions. These hydrogels exhibited improved rheological properties, which were easily tunable, and revealed a rapid self-healing behavior upon rupture. Moreover, boronate ester bonds enabled the fabrication of reactive oxygen species-responsive and shear-thinning gels that can be administered in situ and respond to the oxidation state of the surrounding microenvironment. Importantly, due to the catalyst-free and mild-crosslinking conditions, the generated laminarin-PBA/PVA hydrogels did not show toxicity upon direct contact with preosteoblasts for up to 48 h, and thus constitute a promising platform for tissue engineering and drug delivery applications.

Introduction

Polysaccharides of natural origin represent a unique source of intrinsically biodegradable and biocompatible materials with numerous biomedical applications, including drug delivery systems, 3D/4D bioprinting, soft robotics, bioelectronics, tissue engineering, and regenerative medicine [1–4].

Among the myriad of natural sources available for the sustainable extraction of biorelevant compounds, the sea is undoubtedly one of the most attractive because it constitutes a renewable reservoir of a variety of polysaccharides with fundamental physicochemical features [5]. To date, several types of biopolymers of marine origin, including alginic acid, chitin/chitosan, carrageenan, hyaluronan, and agar,

have been widely explored. Due to their chemical versatility and cost-effectiveness, these polysaccharides have been processed into biomimetic biomaterials of diverse forms (e.g., particles, films, fibers, sponges, and hydrogels) and nano-to-macro dimensions [6, 7]. Such biofunctional platforms constitute valuable building blocks for advancing bottom-up tissue engineering strategies that better recapitulate the native bioarchitecture of living systems through biomaterials and cell synergies [8].

Among marine-derived biomaterials, polysaccharides extracted from brown algae, such as alginic acid (alginate) and fucoidan, have numerous applications in the cosmetic, food, and biopharmaceutical industries. In addition, those seaweeds are also a rich source of bioactive laminarans (laminarin/leucosin), which can constitute up to 35% of the dry content depending on the surrounding habitat, species, and extraction procedure [9].

Laminarin is a particularly interesting storage β -glucan that essentially constitutes a food reserve in macroalgae. This biopolymer can be sustainably extracted from different seaweed species, such as *Laminaria digitata*, *Laminaria hyperborea*, and *Eisenia bicyclis* [9]. In particular, the degree of branching in the backbone of laminarin from *E. bicyclis* generally comprises β -(1,3) and β -(1,6) in the main chain and occasional β -(1,6) side chain branches in the O-6

Supplementary information The online version of this article (<https://doi.org/10.1038/s41428-020-0348-3>) contains supplementary material, which is available to authorized users.

✉ João F. Mano
jmano@ua.pt

¹ CICECO–Aveiro Institute of Materials, Department of Chemistry, University of Aveiro, 3810-193 Aveiro, Portugal

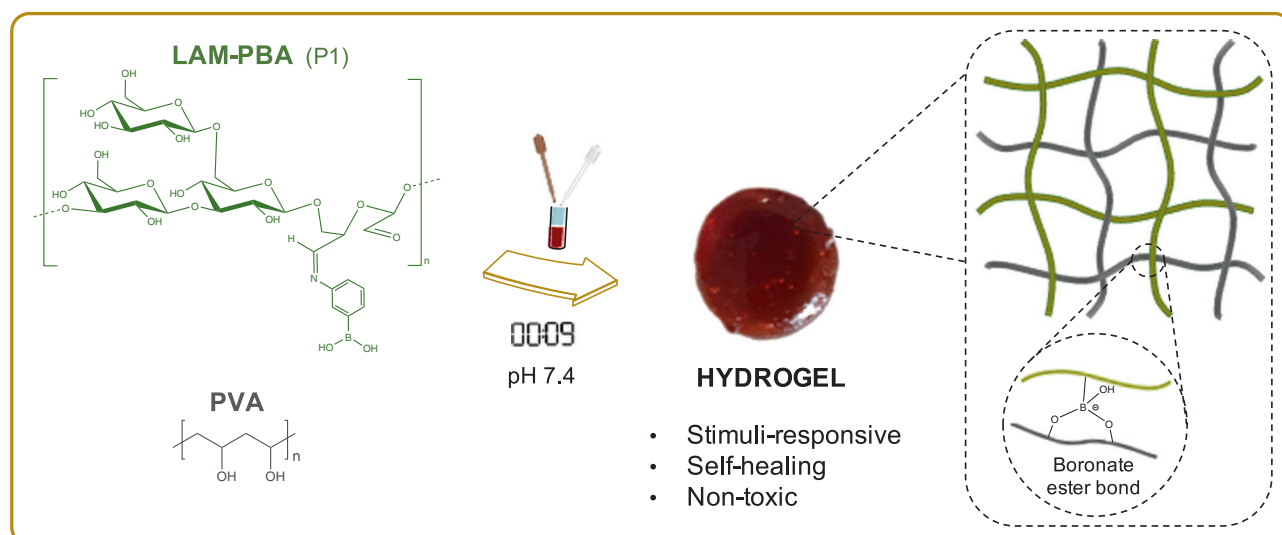


Fig. 1 Schematic representation of hydrogels fabrication via boronate ester crosslinking with PVA

position [10]. This unique structure dictates its water solubility, and a higher degree of branching is more desirable for biomedical applications because it allows dissolution in both hot and cold water [11].

The intrinsic anticoagulant, antioxidant, and immunostimulatory/anti-inflammatory activities of laminarin, which are associated with its biodegradable and chemically versatile backbone, render it a highly attractive biomaterial [12]. However, its lower viscosity and inability to gel compared with alginate has limited its processing into hydrogels, fibers, or particle-based systems. To overcome these limitations and improve its (bio-)functionality/reactivity, laminarin was chemically modified with pendant methacrylic anhydride moieties that react with hydroxyl groups under mild conditions [13]. Using this strategy, the researchers obtained a UV-responsive laminarin-methacrylate derivative that was rapidly photocrosslinked into a mechanically robust and cytocompatible hydrogel. Moreover, this photoreactive derivative has been used for the microfluidic-assisted fabrication of cell-adhesive multifunctional laminarin microparticles [14]. Recent studies have also indicated that chemical modification of the reductive end-sugar of laminarin enables its grafting into hydrophobic polymer backbones and the production of polysaccharide-*b*-polypeptide block copolymers [15]. Hence, the researchers were able to generate small nanoparticles that take advantage of the interaction of laminarin with Dectin-1 receptors for the targeting of immune system cells, such as macrophages. These studies suggest that pristine laminarin constitutes a chemically versatile slate for grafting multifunctional moieties that impart distinctive physicochemical properties.

Taking the above-mentioned results into consideration, biorthogonal and dynamic chemistries can be considered highly attractive strategies for extending the available toolbox of β -glucan-based bioactive materials and exploring new biomedical applications. In addition, it is important to emphasize that its high solubility in organic solvents, including DMSO and DMF, makes laminarin a highly valuable polysaccharide for straightforward chemical modifications [16]. This feature is particularly advantageous because other widely used marine-derived polymers, such as alginate or hyaluronan, require additional and labor-intensive processing into tetrabutyl ammonium salt for organic solvent-based chemical modifications [17].

From this standpoint, biofunctional compounds that allow the development of dynamic and microenvironment-responsive biomaterials provide numerous advantages in comparison with their static, unidirectional photocrosslinkable counterparts [18]. A particularly interesting type of dynamic covalent crosslinking is the formation of reversible boronate ester bonds (in a pH-dependent manner) between boronic acids and *cis*-diol-containing moieties, such as those found in polyols, catechols, and carbohydrates [19]. The typical applications of boronic-functionalized materials include electrochemical and optical sensors, stimuli-responsive hydrogels, insulin delivery systems, and cell culture and capture [20–26]. The polymer networks formed by boronate ester bonds are not permanently rigid but rather transient and can restructure dynamically after disruption, and the interplay between the two functional groups is thus pivotal for self-healing material design [27, 28].

The functionalization of laminarin with boronic acid has yet to be reported, and its successful inclusion is likely to provide innovative applications for this material. Herein, we

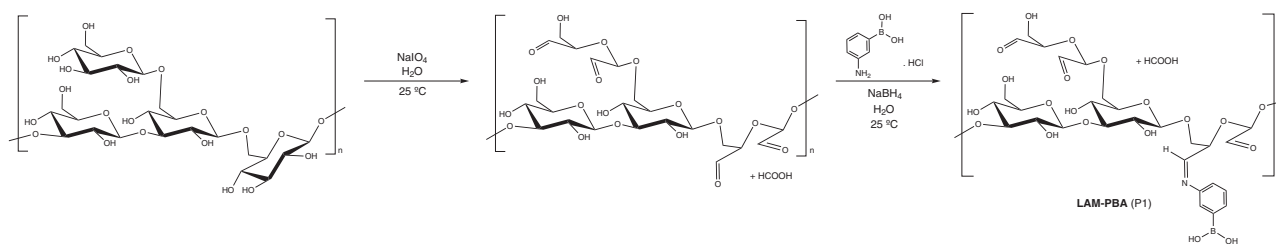


Fig. 2 Functionalization of laminarin with phenylboronic acid (two-pot reaction)

123 describe the modification of laminarin derived from *E.*
 124 *bicyclis* with boronic acid groups. The resulting biopolymer
 125 maintained its high water solubility and enabled conjuga-
 126 tion with diol-rich poly(vinyl alcohol) (PVA), a bio-
 127 compatible and easy-to-handle polymer, via catalyst-free
 128 boronate esterification (Fig. 1). This unique crosslinking
 129 resulted in the simple and rapid preparation of hydrogels at
 130 physiological pH that exhibited self-healing and shear-
 131 thinning properties, responsiveness to reactive oxygen
 132 species (ROS) and cytocompatibility. The newly synthe-
 133 sized derivative represents a next-generation laminarin-
 134 based biopolymer that will have diverse applications in the
 135 fields of drug delivery and tissue engineering.

136 Experimental procedure

137 Synthesis of LAM-PBA (P1)

138 Phenylboronic acid-modified laminarin (LAM-PBA) was
 139 synthesized via a two-step procedure (Fig. 2). First, lami-
 140 narin from *E. bicyclis* (500 mg, 0.617 mmol) and sodium
 141 periodate (440 mg, 2 mmol) were dissolved in 5 mL of
 142 ultrapure water. The mixture was maintained at the room
 143 temperature in the dark for 5 h under magnetic stirring, and
 144 ethylene glycol (117 μ L) was then added to quench the
 145 unreacted aldehyde groups. The resulting biopolymer
 146 exhibited an oxidation degree of *ca.* 53%, as previously
 147 demonstrated [29], was purified by dialysis against water
 148 for 3 days at the room temperature and freeze-dried (Telstar
 149 LyoQuest). Partially oxidized laminarin (190 mg,
 150 0.234 mmol) and 3-aminophenylboronic acid hydrochloride
 151 (76 mg, 0.438 mmol) were then dissolved in ultrapure water
 152 (8 mL), and sodium borohydride (166 mg) in methanol was
 153 then added to the flask. The reaction was allowed to con-
 154 tinue for 8 h in the dark at the room temperature. The
 155 mixture was dialyzed and freeze-dried to obtain a pink
 156 powder (yield \sim 89%). Polymer P1 was then characterized
 157 by ^1H NMR spectroscopy by using a Bruker Advance III
 158 spectrometer (Bruker BioSpin GmbH Rheinstetten,
 159 Deutschland) operating at 300.13 MHz (University of
 160 Aveiro, Portuguese NMR Network-PTNMR). Samples

were dissolved in deuterated water (D_2O), placed in 5 mm
 tubes and spectra were acquired with 256 scans at 298 K.
 The data were processed using the MestReNova
 v6.0.2 software.

165 Hydrogel fabrication

166 Hydrogels ($\text{P1}_5\text{-PVA}_{2.5/3.7/5}$) were prepared by the
 167 mechanical mixing of 10% (w/v) P1 and 5%/7.5%/10% (w/
 168 v) PVA solutions (PBS, pH 7.4) at equal proportions to
 169 ensure homogeneity. The gelation time at the room tem-
 170 perature was monitored using the vial inversion test, and the
 171 gelation process was completed within 10 s.

172 The microstructure of the gels was examined by scanning
 173 electron microscopy (SEM). Prior to examination, the
 174 samples were freeze-dried, cross-sectioned, and sputter-
 175 coated with gold (Hitachi SU-70, Hitachi Ltd, Tokyo,
 176 Japan).

177 Swelling kinetics and degradation tests

178 The hydrogels (m_i) were immersed in PBS (pH 7.4) and
 179 incubated at 25 $^\circ\text{C}$ for 48 h. At predefined time intervals, the
 180 samples ($n = 3$) were removed, gently blotted with filter
 181 paper and weighed (m_f). The swelling ratio was determined
 182 according to the following equation:

$$R(\%) = \frac{m_f - m_i}{m_i} \times 100.$$

185 In addition, the responsiveness of the gels to ROS was
 186 assessed by immersing the disks ($d \approx 10$ mm) in 2 mL of
 187 1 mM hydrogen peroxide (H_2O_2) to calculate the weight
 188 loss over time [30, 31].

189 Mechanical characterization and self-healing 190 evaluation

191 Rheological studies were performed using a Kinexus lab+
 192 rotational rheometer (Malvern) equipped with a stainless-
 193 steel parallel plate geometry. To this end, oscillatory strain
 194 amplitude sweep measurements were performed at a fre-
 195 quency of 1 Hz to determine the linear viscoelastic region

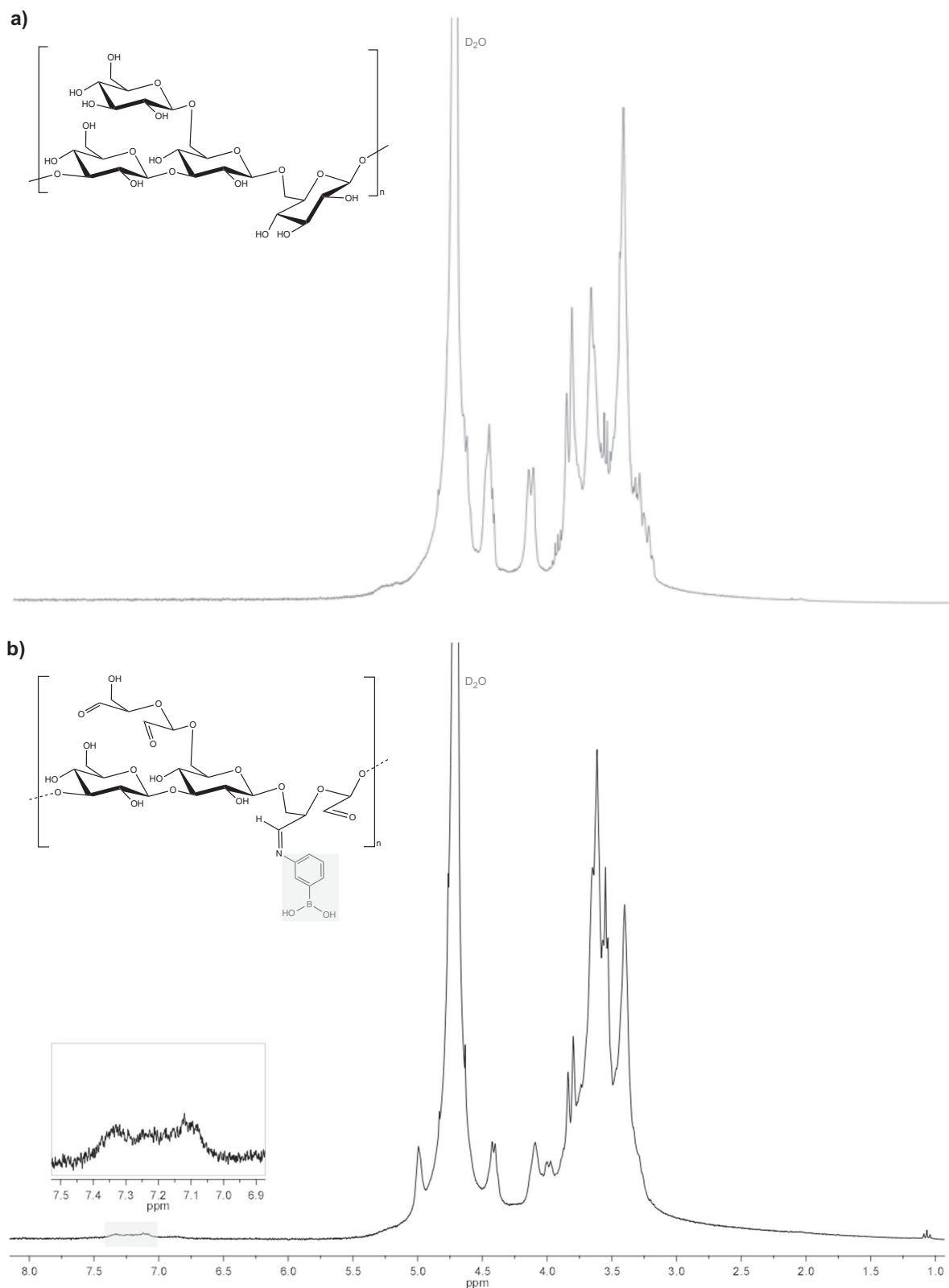


Fig. 3 ^1H NMR spectra of **a** laminarin and **b** LAM-PBA (P1) in D_2O

196 (LVR). Oscillatory frequency sweep measurements were
197 then conducted at a constant strain amplitude of 1% to

measure the storage (G') and loss (G'') moduli. Shear rate
198 ramp tests were performed to evaluate the shear-thinning
199

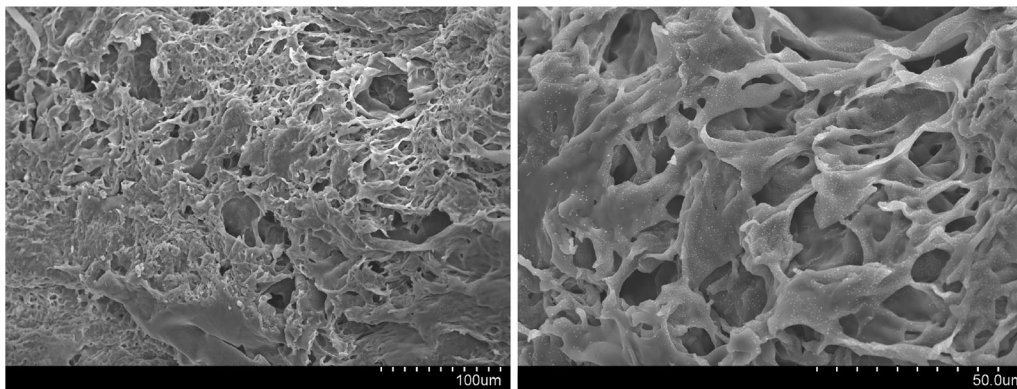


Fig. 4 SEM morphology of freeze-dried P1₅-PVA_{2.5} gels: cross-sectional images at two magnifications

200 profile. Three fresh samples were used for each measure-
201 ment, and the average results are reported.

202 The self-healing ability of the hydrogels was quantita-
203 tively assessed by dynamic rheology. The samples were
204 cleaved into two pieces and brought back into contact, and
205 the recovery of their moduli was then monitored. The
206 alternate step strain sweep response of the gels was mea-
207 sured at 25 °C and 1 Hz by switching from a strain value of
208 1% to a value of 100/200%. The self-healing efficiency was
209 calculated as the ratio of G' of the healed gels to the original
210 modulus (after two cycles).

211 Cell culture and cytotoxicity assays

212 The MC3T3-E1 (ATCC[®] CRL-2593[™]) preosteoblast cell
213 line was cultured at 37 °C under a 5% CO₂ humidified
214 atmosphere in α -MEM culture medium supplemented with
215 10% (v/v) FBS and 1% antibiotic-antimycotic solution. The
216 cells were passaged every 2–3 days once they reached
217 80–90% confluency and reseeded prior to use.

218 The MC3T3-E1 cells were plated on a 48-well plate at a
219 density of 5×10^4 cells/mL. Prior to the assay, hydrogels
220 were prepared as described above, sterilized by exposure to
221 UV light for 15 min, and then incubated for 48 h in direct
222 contact with the cells. The metabolic activity was assessed
223 at different time points using the AlamarBlue[™] assay.
224 Briefly, the cells were incubated with α -MEM containing
225 10% (v/v) AlamarBlue[™] reagent, and after 4 h, the fluo-
226 rescence intensity of the medium was detected at excitation/
227 emission wavelengths of 540/590 nm using a multimode
228 microplate reader (Synergy HTX, BioTek Instruments). The
229 cell viability values are presented as percentages relative to
230 the untreated control cells.

231 Statistical analysis

232 The data are presented as the mean \pm standard deviation
233 (SD) and analyzed using GraphPad Prism software. The

234 statistical significance of the differences was evaluated by
235 one-way ANOVA, and the level of significance was set to a
236 probability $*p < 0.05$.

237 Results and discussion

238 Synthesis and characterization of LAM-PBA (P1)

239 Laminarin was functionalized with a PBA group for the first
240 time via a two-step reaction and characterized by proton
241 nuclear magnetic resonance (¹H NMR). Due to its high
242 abundance of hydroxyl groups, laminarin exhibits high
243 solubility in water and polar solvents, and they can be used
244 for the insertion of functional groups. Initially, laminarin
245 was modified via C-3 and C-4 *cis*-diols selective scission
246 with sodium periodate [32]. The successful oxidation of
247 laminarin allowed the synthesis of an amine-reactive deri-
248 vative, as we previously demonstrated [29]. This approach
249 can be used to functionalize the backbone of laminarin with
250 virtually any biofunctional amine-containing motifs. The
251 chemical composition of polymer P1 could be verified by
252 observing the typical chemical shifts below 5 ppm corre-
253 sponding to the β -D-glucans backbone [33, 34] and the
254 characteristic aromatic peak of PBA at ~ 7.0 – 7.4 ppm, which
255 was not present in pristine laminarin (Fig. 3). This strategy
256 substantially expands the framework of laminarin deriva-
257 tives that can be synthesized according to the desired phy-
258 sicochemical properties.

259 Hydrogel preparation

260 Burgundy-colored hydrogels with different concentration
261 ratios (P1₅-PVA_{2.5/3.7/5}) were prepared within 10 s of mix-
262 ing precursor aqueous solutions of P1 and PVA at pH 7.4,
263 and the formation of these hydrogels was driven by the
264 formation of covalent, albeit reversible, boronate ester
265 bonds between the boronic acid residues of laminarin and

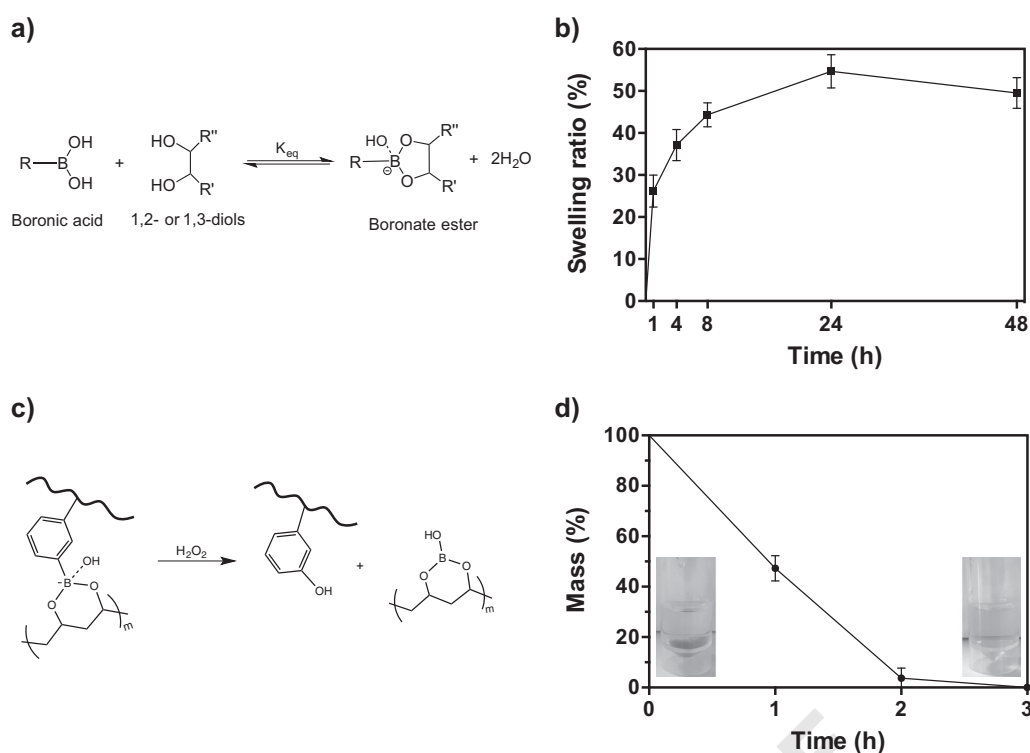


Fig. 5 a Mechanism of the complexation of boronic acid and diol for the formation of cyclic boronate ester in aqueous conditions. **b** Swelling ratio of P1₅-PVA_{2.5} hydrogel in PBS (pH 7.4) at 25 °C. **c**

Schematic of hydrogel degradation upon exposure to H₂O₂. **d** Degradation profile of the gel in 1 mM H₂O₂ solution (mean ± SD from triplicates)

266 the diols of PVA [28, 35]. Preliminary experiments using
 267 different concentrations of the polymers were performed to
 268 determine the minimum polymer feed required for the for-
 269 mation of self-standing hydrogels and the P1₅-PVA_{2.5} for-
 270 mulation was selected for further experiments (Table S1).
 271 SEM images of the P1₅-PVA_{2.5} hydrogel, which are
 272 depicted in Fig. 4, illustrate a typical micron-sized porous
 273 network. Although the formation of boronate ester com-
 274 plexes favorably occurs at pH 9 (pK_a ≈ 8.8), a sufficient
 275 amount of ionizable boronic acid groups that bind to *cis*-
 276 diols present on PVA are present at physiological condi-
 277 tions (pH 7.4) (Fig. 5a) [36]. The addition of unmodified
 278 laminarin to PVA (under the same experimental conditions)
 279 did not result in the formation of any hydrogels, as
 280 expected.

281 Swelling kinetics and stimuli responsiveness

282 The polymeric network was not in equilibrium with the
 283 medium, i.e., the hydrogels were expected to still exhibit
 284 additional water uptake after crosslinking, and thus, the
 285 swelling kinetics of P1₅-PVA_{2.5} gels were assessed for 48 h.
 286 As shown in Fig. 5b, the hydrogels exhibited a moderate
 287 swelling capacity (*ca.* 55%) and reached equilibrium after
 288 24 h of immersion in PBS (pH 7.4), which indicates that the
 289 stability of the hydrogels.

290 Methods for the selective delivery of therapeutic or
 291 diagnostic agents to sites undergoing oxidative stress would
 292 prove useful for various diseases characterized by high
 293 concentrations of ROS [31]. These species are normally
 294 produced during biological processes and exhibit significant
 295 oxidative potential, particularly in tumor tissues. In this
 296 sense, ROS-responsive materials comprising boronic acid
 297 motifs have been explored for the development of fluores-
 298 cent probes, imaging agents, and oxidation-sensitive
 299 carriers [30]. In particular, species such as H₂O₂ can oxi-
 300 dize the boronate ester complex by inserting an oxygen
 301 atom in the C–B bond, which induces the formation of
 302 borate esters and hydroxybenzyl derivatives (Fig. 5c) [37].
 303 Figure 5d shows the effect of ROS on P1₅-PVA_{2.5} gel
 304 stability. After 3 h, the hydrogel was completely degraded
 305 in the presence of 1 mM H₂O₂, and this degradation was
 306 driven by irreversible network rupture.

307 Mechanical properties and self-healing

308 We studied the dynamic rheological properties of the
 309 hydrogels obtained with representative P1 and PVA con-
 310 centrations (see Fig. 6a–c). Initially, oscillatory strain
 311 sweeps were performed at the room temperature to deter-
 312 mine the LVR. We observed an increase in the storage (G')
 313 and loss (G'') moduli crossover strain value, which is
 314

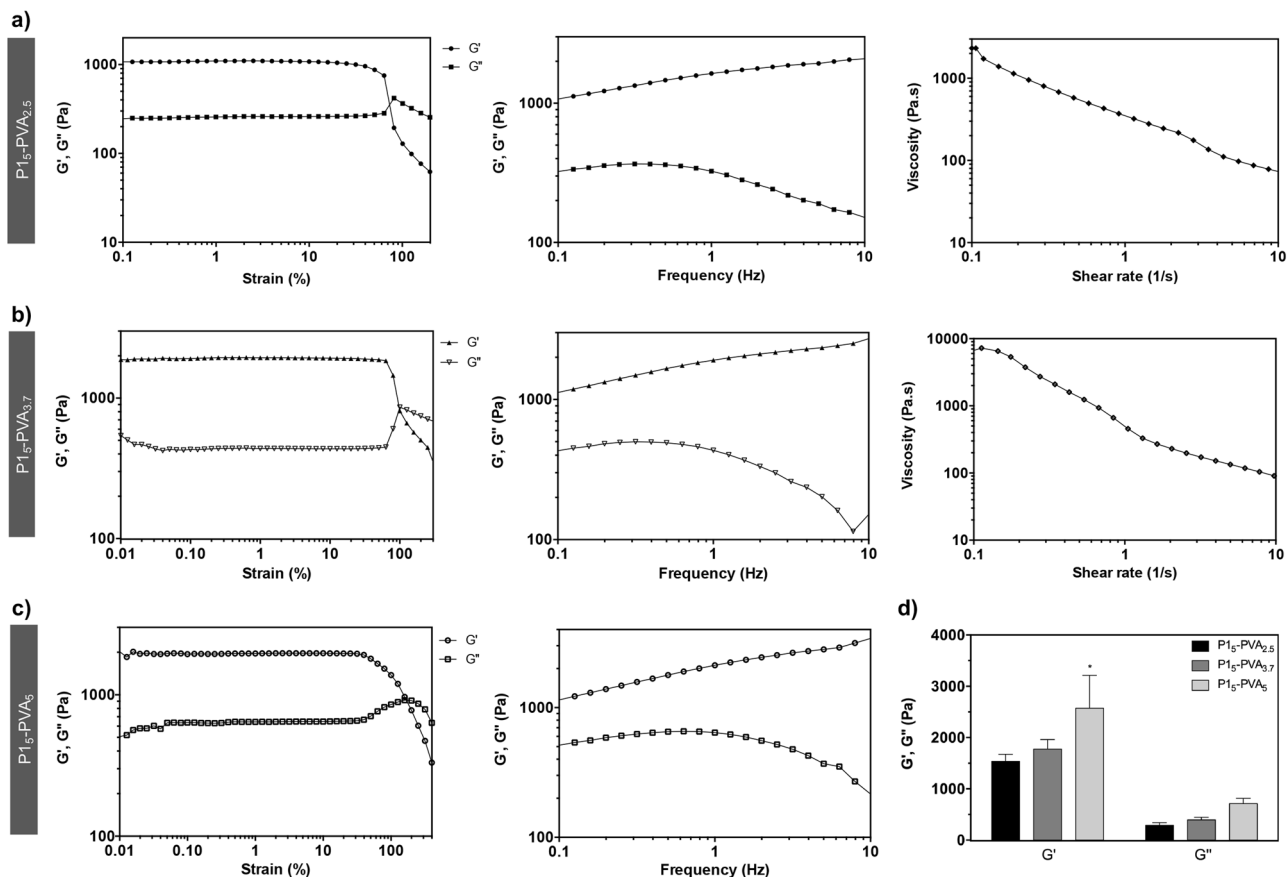


Fig. 6 Rheological properties of **a** P_{15} -PVA_{2.5}, **b** P_{15} -PVA_{3.7}, and **c** P_{15} -PVA₅. Strain sweep measurements of gels at fixed 1 Hz (left), variation in the G' and G'' moduli with frequency (middle), and shear-

thinning behavior at 25 °C (right). **d** Comparison of G' and G'' values of selected gels at 1 Hz as function of the PVA concentration (mean ± SD)

314 required for disruption of the polymer network, at higher
315 PVA concentrations.

316 It is well known that the viscoelasticity of a material and
317 mechanotransduction might affect cellular responses
318 [38, 39]. Frequency sweep measurements were thus per-
319 formed within this region to evaluate the mechanical
320 strength of the constructs. The gels demonstrated a minor
321 frequency-dependent viscoelastic behavior, but the G'
322 was greater than the G'' at all regimes, which is indicative of a
323 gel-like character (elastic component is dominant). The
324 influence of the PVA concentration on the rheological
325 properties of the hydrogels was also evaluated by compar-
326 ing the G' and G'' values (Fig. 6d). Reducing the con-
327 centration from 5 to 2.5% decreased the G' from *ca.* 2500
328 to 1500 Pa, likely due to the lower crosslinking density, which
329 impacts the mechanical properties; a similar trend was
330 found for G'' . As expected, the stiffness of the gels
331 improved with increases in the concentration of PVA
332 polymer.

333 Moreover, as the dynamic boronate esters in the network
334 start to disrupt, the viscosity of the gels (P_{15} -PVA_{2.5/3.7})

335 decreased with increasing shear rate, following the power
336 law model, which is indicative of a shear-thinning profile.

337 The self-healing behavior of freshly prepared
338 P_{15} -PVA_{2.5} gels was visually investigated. To this end, the
339 hydrogels were cut in half, as displayed in Fig. 7a, and after
340 the pieces were directly brought into contact, their healing
341 into one integral piece was observed within 30 min in the
342 absence of any external stimulus, although the cut interface
343 was still vaguely visible. To investigate the hydrogel self-
344 healing capability in more detail, strain sweep measure-
345 ments were carried out to evaluate the autonomous recovery
346 of their rheological properties (Figs. 7c and S1). At low
347 strain values (1%), the G' value was higher than the G''
348 value, but the application of a high-magnitude strain (100%)
349 to the gel induced an inversion of the moduli due to dis-
350 ruption of the network (large deformation); after removal of
351 the high strain, both the G' and G'' values of the gel rapidly
352 recovered to their original values without any noticeable
353 loss over time (*ca.* 99% recovery), which differs from other
354 healing mechanisms [40, 41]. These interesting self-healing
355 properties under mild conditions are mainly imparted to the
356 transient dissociation of the dynamic reversible boronate
357

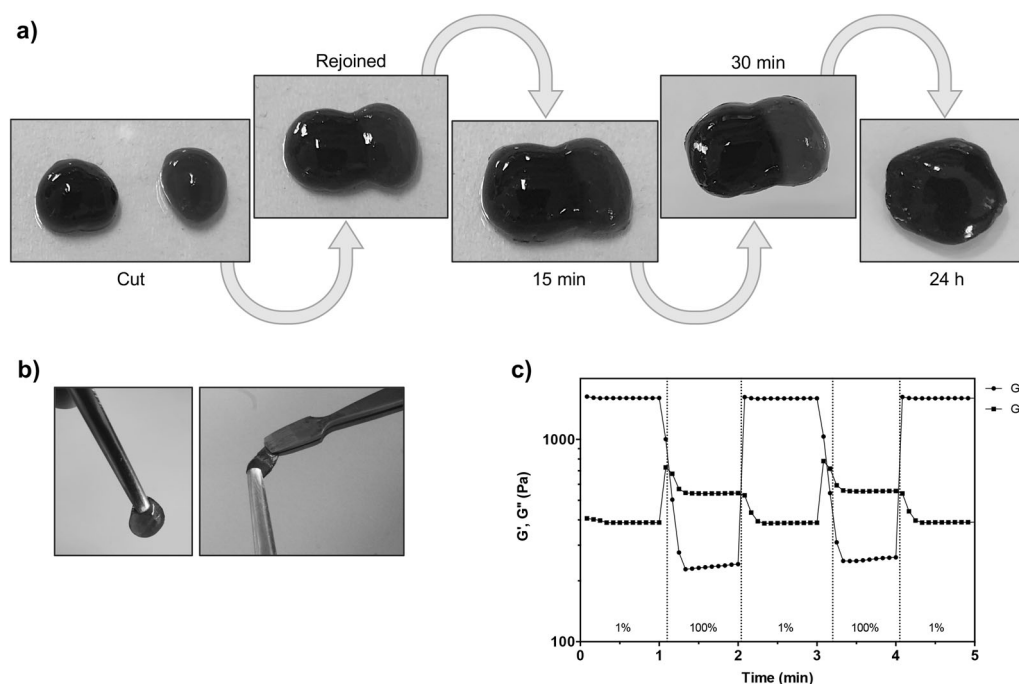


Fig. 7 **a** Hydrogel self-healing behavior: two pieces (with and without green dye for better contrast) were mechanically rejoined, and their recovery process was monitored. **b** The healed hydrogel could maintain its integrity and withstand deformation. **c** A dynamic oscillatory

test was employed by shearing the $P1_5$ - $PVA_{2.5}$ samples at constant 1 Hz, from 1 to 100% strain (alternate) and by monitoring the variations in the G' and G'' values

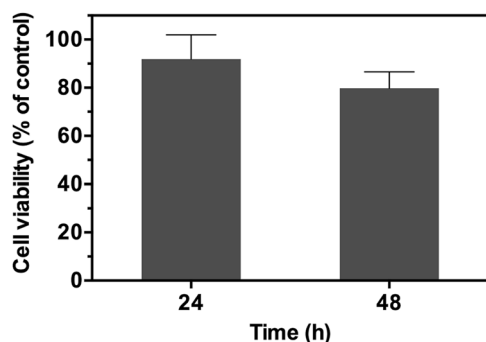


Fig. 8 Metabolic activity of MC3T3-E1 preosteoblast cells incubated with the $P1_5$ - $PVA_{2.5}$ gel. The activity was determined using the AlamarBlue™ assay. The cell viability data are shown as percentages with respect to the untreated (control) cells (mean \pm SD from triplicates)

357 ester complexes, which upon reforming, allow the rapid
358 (<1 min) and efficient rearrangement of the polymeric
359 network.

360 Cytocompatibility evaluation

361 After the physicochemical and mechanical characterization
362 of the polymeric hydrogels, we performed in vitro toxicity
363 studies to investigate the effect of the $P1_5$ - $PVA_{2.5}$ gel on the
364 metabolic activity of MC3T3-E1 cells as a model. As

observed in Fig. 8, the gels did not exhibit any toxicity after 365
48 h, with ~80% of the cells remaining viable. 366

367 Conclusion

368 In conclusion, this study demonstrates the first functionali-
369 zation of laminarin with PBA moieties through a simple and
370 cost-effective two-pot approach. This biopolymer was then
371 used for the rapid fabrication of versatile hydrogels under
372 physiological conditions based on the dynamic formation of
373 covalent boronate ester bonds between the boronic acids in
374 the backbone and the *cis*-diols of PVA. The 3D constructs
375 exhibited tunable mechanical properties with shear thinning
376 and rapid self-healing characteristics. This platform was
377 found to be cytocompatible for culturing a preosteoblastic
378 model cell line, and its biocompatibility will likely enable
379 the inclusion of different cell types. Furthermore, the
380 hydrogels were confirmed to be responsive to ROS and
381 noncytotoxic, and these findings pave the way for their
382 application in biomedicine as drug delivery carriers and/or
383 bioinks for tissue engineering.

384 **Acknowledgements** This work was supported by the European
385 Research Council (ERC-2014-ADG-669858) and project CICECO-
386 Aveiro Institute of Materials, UIDB/50011/2020 & UIDP/50011/2020,
387 financed by national funds through the Portuguese FCT/MCTES. The
388 NMR spectrometer is part of the National NMR Network (PTNMR)

389 and partially supported by Infrastructure Project N° 022161 (co-
 390 financed by FEDER through COMPETE 2020, POCI and PORE, and
 391 FCT through PIDDAC). This work was also funded by the Programa
 392 Operacional Competitividade e Internacionalização (POCI), in the
 393 component FEDER, and by national funds (OE) through FCT/MCTES
 394 within the scope of the project MARGEL (PTDC/BTM-MAT/31498/
 395 2017). VMG acknowledges funding in the form of a Junior Research
 396 contract under the scope of project PANGEIA (PTDC/BTM-SAL/
 397 30503/2017).

398 Compliance with ethical standards

399 **Conflict of interest** The authors declare that they have no conflict of
 400 interest.

401 **Publisher's note** Springer Nature remains neutral with regard to
 402 jurisdictional claims in published maps and institutional affiliations.

403 References

- 404 1. Cardoso JM, Costa RR, Mano JF. Marine origin polysaccharides
 405 in drug delivery systems. *Mar Drugs* 2016;14:E34. pii
- 406 2. Zhu T, Mao J, Cheng Y, Liu H, Lv L, Ge M, et al. Recent progress
 407 of polysaccharide-based hydrogel interfaces for wound healing
 408 and tissue engineering. *Adv Mater Interfaces*. 2019;6:1900761.
- 409 3. Liu J, Sun L, Xu W, Wang Q, Yu S, Sun J. Current advances and
 410 future perspectives of 3D printing natural-derived biopolymers.
 411 *Carbohydr Polym* 2019;207:297–316.
- 412 4. Kuang Y, Chen C, Cheng J, Pastel G, Li T, Song J, et al.
 413 Selectively aligned cellulose nanofibers towards high-performance
 414 soft actuators. *Extrem Mech Lett*. 2019;29:100463.
- 415 5. Silva TH, Alves A, Ferreira BM, Oliveira JM, Reys LL, Ferreira
 416 RJF, et al. Materials of marine origin: a review on polymers and
 417 ceramics of biomedical interest. *Int Mater Rev*. 2012;57:276–306.
- 418 6. Mano JF. Designing biomaterials for tissue engineering based on
 419 the deconstruction of the native cellular environment. *Mater Lett*
 420 2015;141:198–202.
- 421 7. Joshi S, Eshwar S, Jain V. Marine-derived biomaterials for tissue
 422 engineering applications. In: Choi AH, Ben-Nissan B, editors.
 423 Singapore: Springer; 2019. p. 443–87.
- 424 8. Gaspar VM, Lavrador P, Borges J, Oliveira MB, Mano JF.
 425 Advanced bottom-up engineering of living architectures. *Adv*
 426 *Mater* 2020;32:1903975.
- 427 9. Kadam SU, Tiwari BK, O'Donnell CP. Extraction, structure and
 428 biofunctional activities of laminarin from brown algae. *Int J Food*
 429 *Sci Tech*. 2015;50:24–31.
- 430 10. Ojima T, Rahman MM, Kumagai Y, Nishiyama R, Narsico J,
 431 Inoue A. Methods in enzymology. In: Moore BS, editor. Aca-
 432 **Q7**ademic Press; 2018. p. 457–97.
- 433 11. Rioux L-E, Turgeon SL. Seaweed sustainability. In: Tiwari BK,
 434 Troy DJ, editors. Academic Press; 2015. p. 141–92.
- 435 12. Zargarzadeh M, Amaral AJR, Custódio CA, Mano JF. Biomedical
 436 applications of laminarin. *Carbohydr Polym* 2020;232:115774.
- 437 13. Custódio CA, Reis RL, Mano JF. Photo-cross-linked laminarin-
 438 based hydrogels for biomedical applications. *Biomacromolecules*.
 439 2016;17:1602–9.
- 440 14. Martins CR, Custódio CA, Mano JF. Multifunctional laminarin
 441 microparticles for cell adhesion and expansion. *Carbohydr Polym*.
 442 2018;202:91–8.
- 443 15. Duan H, Donovan M, Foucher A, Schultze X, Lecommandoux S.
 444 Multivalent and multifunctional polysaccharide-based particles for
 445 controlled receptor recognition. *Sci Rep*. 2018;8:14730.

- 446 16. Shin HJ, Oh SJ, Kim SI, Won Kim H, Son J-H. Conformational
 447 characteristics of β -glucan in laminarin probed by terahertz
 448 spectroscopy. *Appl Phys Lett*. 2009;94:111911.
- 449 17. Palumbo FS, Fiorica C, Pitarresi G, Giorgi M, Abramo F, Gulino
 450 A, et al. Construction and evaluation of sponge scaffolds from
 451 hyaluronic acid derivatives for potential cartilage regeneration. *J*
 452 *Mater Chem B*. 2014;2:3243–53.
- 453 18. Marco-Dufort B, Tibbitt MW. Design of moldable hydrogels for
 454 biomedical applications using dynamic covalent boronic esters.
 455 *Mater Today Chem*. 2019;12:16–33.
- 456 19. Springsteen G, Wang B. A detailed examination of boronic
 457 acid–diol complexation. *Tetrahedron*. 2002;58:5291–300.
- 458 20. Pasparakis G, Vamvakaki M, Krasnogor N, Alexander C.
 459 Diol–boronic acid complexes integrated by responsive polymers
 460 —a route to chemical sensing and logic operations. *Soft Matter*.
 461 2009;5:3839–41.
- 462 21. Guan Y, Zhang Y. Boronic acid-containing hydrogels: synthesis
 463 and their applications. *Chem Soc Rev*. 2013;42:8106–21.
- 464 22. Amaral AJR, Pasparakis G. Macromolecular cell surface engi-
 465 neering for accelerated and reversible cellular aggregation. *Chem*
 466 *Commun*. 2015;51:17556–9.
- 467 23. Amaral AJR, Pasparakis G. Rapid formation of cell aggregates
 468 and spheroids induced by a “smart” boronic acid copolymer. *ACS*
 469 *Appl Mater Interfaces*. 2016;8:22930–41.
- 470 24. Brooks WLA, Sumerlin BS. Synthesis and applications of boronic
 471 acid-containing polymers: from materials to medicine. *Chem Rev*.
 472 2016;116:1375–97.
- 473 25. Pettignano A, Grijalvo S, Häring M, Eritja R, Tanchoux N,
 474 Quignard F, et al. Boronic acid-modified alginate enables direct
 475 formation of injectable, self-healing and multistimuli-responsive
 476 hydrogels. *Chem Commun*. 2017;53:3350–3.
- 477 26. Quirós J, Amaral AJR, Pasparakis G, Williams GR, Rosal R.
 478 Electrospun boronic acid-containing polymer membranes as
 479 fluorescent sensors for bacteria detection. *React Funct Polym*.
 480 2017;121:23–31.
- 481 27. Amaral AJR, Pasparakis G. Stimuli responsive self-healing
 482 polymers: gels, elastomers and membranes. *Polym Chem*.
 483 2017;8:6464–84.
- 484 28. Amaral AJR, Emamzadeh M, Pasparakis G. Transiently malleable
 485 multi-healable hydrogel nanocomposites based on responsive
 486 boronic acid copolymers. *Polym Chem*. 2018;9:525–37.
- 487 29. Lavrador P, Gaspar VM, Mano JF. Mechanochemical patternable
 488 ecm-mimetic hydrogels for programmed cell orientation. *Adv*
 489 *Health Mater*. 2020. <https://doi.org/10.1002/adhm.201901860>
- 490 30. Saravanakumar G, Kim J, Kim WJ. Reactive-oxygen-species-
 491 responsive drug delivery systems: promises and challenges. *Adv*
 492 *Sci*. 2017;4:1600124.
- 493 31. Ye H, Zhou Y, Liu X, Chen Y, Duan S, Zhu R, et al. Recent
 494 advances on reactive oxygen species-responsive delivery and
 495 diagnosis system. *Biomacromolecules*. 2019;20:2441–63.
- 496 32. Kristiansen KA, Poththast A, Christensen BE. Periodate oxidation
 497 of polysaccharides for modification of chemical and physical
 498 properties. *Carbohydr Res*. 2010;345:1264–71.
- 499 33. Kim Y-T, Kim E-H, Cheong C, Williams DL, Kim C-W, Lim S-
 500 T. Structural characterization of β -d-(1→3, 1→6)-linked glucans
 501 using nmr spectroscopy. *Carbohydr Res*. 2000;328:331–41.
- 502 34. Sellimi S, Maalej H, Rekiq DM, Benslima A, Ksouda G, Hamdi
 503 M, et al. Antioxidant, antibacterial and in vivo wound healing
 504 properties of laminarin purified from cystoseira barbata seaweed.
 505 *Int J Biol Macromol*. 2018;119:633–44.
- 506 35. Kitano S, Koyama Y, Kataoka K, Okano T, Sakurai Y. A novel
 507 drug delivery system utilizing a glucose responsive polymer
 508 complex between poly (vinyl alcohol) and poly (N-vinyl-2-pyr-
 509 rolidone) with a phenylboronic acid moiety. *J Controlled Release*.
 510 1992;19:161–70.

- 511 36. Kataoka K, Miyazaki H, Okano T, Sakurai Y. Sensitive glucose-
512 induced change of the lower critical solution temperature of poly
513 [N,N-(dimethylacrylamide)-co-3-(acrylamido)-phenylboronic
514 acid] in physiological saline. *Macromolecule*. 1994;27:1061–2.
- 515 37. Lippert AR, Van de Bittner GC, Chang CJ. Boronate oxidation as
516 a bioorthogonal reaction approach for studying the chemistry of
517 hydrogen peroxide in living systems. *Acc Chem Res*.
518 2011;44:793–804.
- 519 38. Fusco S, Panzetta V, Embrione V, Netti PA. Crosstalk between
520 focal adhesions and material mechanical properties governs cell
521 mechanics and functions. *Acta Biomater*. 2015;23:63–71.
- 533
- 534
- 535
- 536
- 537
- 538
- 539
- 540
- 541
- 542
- 543
- 544
- 545
- 522 39. Marozas IA, Anseth KS, Cooper-White JJ. Adaptable boronate
523 ester hydrogels with tunable viscoelastic spectra to probe time-
524 scale dependent mechanotransduction. *Biomaterials*.
525 2019;223:119430.
- 526 40. Deng G, Li F, Yu H, Liu F, Liu C, Sun W, et al. Dynamic
527 hydrogels with an environmental adaptive self-healing ability and
528 dual responsive sol–gel transitions. *ACS Macro Lett*.
529 2012;1:275–9.
- 530 41. Argun A, Algi MP, Tuncaboylu DC, Okay O. Surfactant-induced
531 healing of tough hydrogels formed via hydrophobic interactions.
532 *Colloid Polym Sci*. 2014;292:511–7.

Graphical Abstract

The functionalization of laminarin with boronic acid groups was described. This biopolymer readily established boronate ester-crosslinked gels with poly(vinyl alcohol) within seconds under physiological conditions. The resultant hydrogels exhibited interesting self-healing properties, reactive oxygen species responsiveness and cytocompatibility.

